AIAA JOURNAL
Vol. 35, No. 1, January 1997

Bifurcation of Low Reynolds Number Flows in Symmetric Channels

Francine Battaglia,* Simon J. Tavener,† Anil K. Kulkarni,‡ and Charles L. Merkle§
Pennsylvania State University, University Park, Pennsylvania 16802

The flowfields in two-dimensional channels with discontinuous expansions are studied numerically to understand how the channel expansion ratio influences the symmetric and nonsymmetric solutions that are known to occur. For improved confidence and understanding, two distinct numerical techniques are used. The general flowfield characteristics in both symmetric and asymmetric regimes are ascertained by a time-marching finite difference procedure. The flowfields and the bifurcation structure of the steady solutions of the Navier–Stokes equations are determined independently using the finite element technique. The two procedures are then compared both as to their predicted critical Reynolds numbers and the resulting flowfield characteristics. Following this, both numerical procedures are compared with experiments. The results show that the critical Reynolds number decreases with increasing channel expansion ratio. At a fixed supercritical Reynolds number, the location at which the jet first impinges on the channel wall grows with the expansion ratio.

Nomenclature

D = outlet height
d = inlet height
E = flux vectors with gradients in the streamwise direction
E_v = viscous flux vectors with gradients in the streamwise direction
F = flux vectors with gradients in the cross-stream direction
F_v = viscous flux vectors with gradients in the cross-stream direction
$\boldsymbol{f}_w$ = matrix of partial derivatives $\partial f_i/\partial x_j$, $i, j = 1, \ldots, n$
J = Jacobian
L = length of channel domain
p = pressure
Q = vector of the conservative primitive variables
$\mathbb{R}$ = set of all real numbers
$\mathbb{R}^N$ = set of all real vectors of dimension N
Re = Reynolds number
Re_c = critical Reynolds number
S = symmetry matrix
t = time
U = contravariant velocity in the ξ direction
u = streamwise velocity component
$\boldsymbol{u}$ = velocity vector
$\bar{u}$ = mean velocity
V = contravariant velocity in the η direction
v = cross-stream velocity component
$\boldsymbol{w}$ = vector of nodal velocity and pressure degrees of freedom
x = streamwise direction
$\boldsymbol{x}$ = position vector
y = cross-stream direction
β = artificial compressibility parameter
Γ = cofficient matrix for time derivative
Γ_p = modified coefficient matrix for time derivative
η = independent variable for cross-stream direction
ν = kinematic viscosity
ξ = independent variable for streamwise direction
τ = independent (pseudo) time variable
ϕ_c = n-dimensional eigenvector of $\boldsymbol{f}_w^c$ corresponding to eigenvalue zero
ψ_c = n-dimensional vector orthogonal to the range of $\boldsymbol{f}_w^c$

Subscripts and Superscripts

c = singular point
0 = regular point

Received May 1, 1996; revision received Sept. 13, 1996; accepted for publication Sept. 13, 1996; also published in *AIAA Journal on Disc*, Volume 2, Number 1.

*Department of Energy Graduate Assistance in Areas of National Need Graduate Fellow, Department of Mechanical Engineering. Student Member AIAA.
†Associate Professor, Department of Mathematics.
‡Professor, Department of Mechanical Engineering.
§Professor, Department of Mechanical Engineering. Member AIAA.

I. Introduction

IT is well known that laminar flows in two-dimensional channels with discontinuous, symmetric expansions can produce either symmetric or nonsymmetric solutions, depending on the value of the Reynolds number as compared with some critical value. Both the intriguing physics of these flows and their importance in engineering applications have attracted considerable previous attention. Experimental investigations of the problem include the work of Durst et al.,[1] Cherdron et al.,[2] and Ouwa et al.[3] These experimental results make clear that the jet produced by the sudden expansion remains symmetrically placed in the channel at low Reynolds numbers but becomes asymmetric at higher values and attaches to either the upper or lower wall. Companion numerical computations of the symmetry-breaking bifurcation point by Fearn et al.[4] and linear stability analyses of flows in symmetric channels by Shapira et al.[5] indicate that this observed experimental behavior occurs at a bifurcation of the Navier–Stokes equations.

The channel expansion ratios considered in these previous studies have been limited to a narrow range of values. In particular, Fearn et al.[4] compared numerical computations of the symmetry-breaking bifurcation point with laboratory experiments for a channel with a 1:3 expansion ratio, whereas Shapira et al.[5] conducted their linear stability analyses for 1:2 and 1:3 expansion ratio channels. In addition, Durst et al.[6] have reported a combined numerical-experimental study of a 1:2 expansion ratio channel. All studies conclude that symmetric flows become unstable as the Reynolds number is increased above a critical value and that steady asymmetric flows develop above this critical condition. We investigate this behavior numerically for a range of expansion ratios, emphasizing the common features of this exchange of stability.

To provide broad understanding of the channel expansion flowfield as well as confidence in the accuracy of the predictions, we use two distinct numerical analyses. First, a time-marching finite difference procedure that includes both time-accurate and steady-state versions is used to investigate the flowfield characteristics above and below the critical Reynolds numbers. By their nature, time-marching procedures cannot reveal the bifurcation point directly, but they can (presumably) predict the flowfield accurately on either side of the

critical condition. For any given computation, the nature of the flow (subcritical or supercritical) cannot be deduced beforehand, but an indication of the bifurcation point can be inferred by starting from one symmetric solution and one nonsymmetric solution and decreasing the distance between them by computing flows at intermediate Reynolds numbers. Not surprisingly, results show that the convergence time gets larger and larger as the critical Reynolds number is approached, thereby leaving some uncertainty in the ultimate value of the critical point. Further, the ability of the time-marching procedure to predict the bifurcation phenomena accurately requires validation. Experimental observations clearly represent one avenue for this purpose, but as experiments can include unavoidable and undetected asymmetries that can bias the results,[4] a bifurcation analysis is used herein as a second independent numerical investigation of the problem.

The bifurcation analysis uses a finite element method and an extended system technique to locate the bifurcation points. The advantage of this analysis is that it determines the symmetry-breaking point directly. The finite element technique also provides complete flowfields for both symmetric and asymmetric solutions, which can then be compared with the time-marching flowfield solutions. Final validation of both methods includes comparisons with experimental measurements.

Of the numerous engineering applications of these types of bifurcating solutions, our particular interest stems from an unsteady, three-dimensional application in which the channel geometry is axisymmetric, rather than planar, in nature. Researchers at the University of Adelaide have experimentally observed a naturally occurring fluid mechanical phenomenon known as a precessing jet. While performing experiments to find ways to improve flame stability of a natural gas burner, Luxton and Nathan[7] discovered that with certain expansion ratios of the nozzle inlet orifice and for sufficiently large flow rates an asymmetric precessing jet developed. No additional devices or moving parts are associated with the burner to produce the swirling flow.[8] Further experiments indicated enhanced combustion and mixing characteristics when a precessing jet burner was used in place of a conventional jet burner. Burners that encourage a precessing jet have been applied to the combustion process, which takes place in an industrial cement kiln, and are currently being used in Australia, the United Kingdom, and the United States.

The paper is structured as follows. The two numerical schemes employed are discussed in Sec. II. Simulations were performed using an artificial compressibility formulation with dual time stepping. The finite element method and an extended system technique were used to compute the bifurcation structure. A detailed discussion of the numerical findings is presented in Sec. III. Results of previously published work are compared with the results reported here. In particular, we compare not only published estimates of the critical Reynolds numbers but also our computed velocity profiles for two supercritical Reynolds numbers for a range of downstream locations, with laser Doppler velocimetry (LDV) measurements. The effects of expansion ratio on the asymmetry of the flow are presented in detail.

II. Numerical Formulations

The problem of interest concerns the flowfield downstream of a sudden enlargement in a planar duct of the type shown in Fig. 1. The flow is taken to be laminar and fully developed prior to the sudden enlargement. We wish to find the velocity and pressure fields $\boldsymbol{u}(\boldsymbol{x}, t)$ and $p(\boldsymbol{x}, t)$, respectively, which satisfy the incompressible Navier–Stokes equations,

$$Re\left(\frac{\partial \boldsymbol{u}}{\partial t} + \boldsymbol{u}\cdot\nabla\boldsymbol{u}\right) = -\nabla p + \Delta\boldsymbol{u} \tag{1}$$

and

$$\nabla\cdot\boldsymbol{u} = 0 \tag{2}$$

in the domain shown in Fig. 1, subject to the boundary conditions described next. We define the Reynolds number as $Re = \bar{u}d/\nu$. Here $\bar{u} = Q/d$, where Q is the volume flux per unit length perpendicular to the x–y plane. The expansion ratio is defined as D/d. The domain length was chosen such that Poiseuille flow was recovered at the downstream end of the channel. This choice implies that an upper bound exists for the maximum Reynolds number that can be simulated accurately on a domain of any given length. A fully developed parabolic velocity profile was specified at the upstream boundary with nonslip boundary conditions imposed along the channel walls. The ambient pressure was specified at the downstream boundary for the numerical simulations. Natural boundary conditions, $p + \partial u/\partial x = 0$ and $\partial v/\partial x = 0$, pertain at the downstream boundary for the finite element computations. In the following, the time-marching solutions are referred to as the simulations, whereas the symmetry breaking solutions are referred to as the bifurcation calculations.

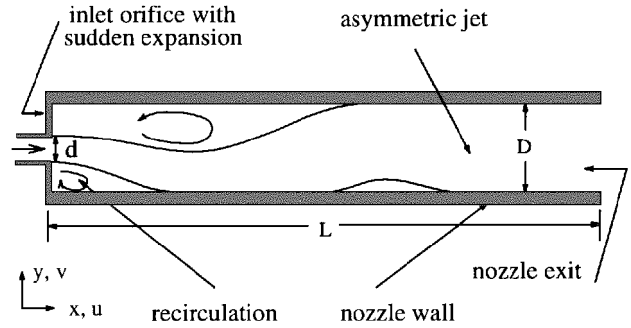

Fig. 1 Schematic of a two-dimensional planar nozzle with an asymmetric jet, flowing from left to right.

A. Simulations

The numerical simulations using the time-marching formulation are obtained by transforming Eqs. (1) and (2) from a Cartesian (x, y) to a generalized coordinate system (ξ, η). When written in conservative form, these become

$$\Gamma\frac{\partial Q}{\partial t} + \frac{\partial}{\partial\xi}(E - E_v) + \frac{\partial}{\partial\eta}(F - F_v) = 0 \tag{3}$$

where

$$\Gamma = \begin{pmatrix} 0 & 0 & 0 \\ 0 & 1 & 0 \\ 0 & 0 & 1 \end{pmatrix}, \qquad Q = \frac{1}{J}\begin{pmatrix} p \\ u \\ v \end{pmatrix}$$

$$E = \begin{pmatrix} U \\ uU + p\xi_x \\ vU + p\xi_y \end{pmatrix}, \qquad F = \begin{pmatrix} V \\ uV + p\eta_x \\ vV + p\eta_y \end{pmatrix}$$

and

$$E_v = \frac{\nu}{J}\left[(\nabla\xi\cdot\nabla\xi)\frac{\partial(JQ)}{\partial\xi} + (\nabla\xi\cdot\nabla\eta)\frac{\partial(JQ)}{\partial\eta}\right]$$

$$F_v = \frac{\nu}{J}\left[(\nabla\xi\cdot\nabla\eta)\frac{\partial(JQ)}{\partial\xi} + (\nabla\eta\cdot\nabla\eta)\frac{\partial(JQ)}{\partial\eta}\right]$$

with

$$U = u\xi_x + v\xi_y$$

$$V = u\eta_x + v\eta_y$$

where all subscripts refer to partial derivatives. By changing the physical time to a pseudotime and redefining the matrix Γ as

$$\Gamma_p = \begin{pmatrix} 1/\beta & 0 & 0 \\ 0 & 1 & 0 \\ 0 & 0 & 1 \end{pmatrix}$$

Eq. (3) becomes the artificial compressibility method,[9] which has been widely used. This change transforms the Euler portion of the system of equations into a set of fully hyperbolic equations, permitting the use of time-marching schemes for either the Euler or Navier–Stokes equations. A complete description of the formulation is given in Ref. 10.

When the artificial compressibility method is used, the equations become physically incorrect in the transient and are only accurate for steady-state flows. Time accuracy can, however, be recovered by combining the artificial compressibility method with a dual time stepping scheme. Specifically, a pseudotime derivative $\Gamma_p \partial Q/\partial \tau$ is added to Eq. (3). The solution in real time is obtained by iterating in pseudotime until convergence is achieved as $\partial Q/\partial \tau \longrightarrow 0$. The physical time derivatives are implicitly discretized using second-order differencing and the spatial derivatives are discretized using central differencing. In the present calculations, a four-stage Runge–Kutta explicit scheme is used to integrate the solution in pseudotime for either steady-state or time-accurate solutions. Further details of the numerics are described in Refs. 10 and 11.

The scheme has been validated against spatial stability theory[12] to ensure accuracy in both space and time. In addition, numerical tests were performed to determine the grid size needed to resolve the flowfield and generate grid-independent solutions in the present problem. Five meshes of 111×111, 256×111, 512×111, 1024×111, and 256×221 grid points were used to determine the accuracy of the solution. Convergence tolerances were also examined by computing a solution to machine accuracy and determining if the solution changed significantly.

B. Bifurcation Calculations

Following a standard finite element development (for example, Ref. 13), the Navier–Stokes equations and appropriate boundary conditions may be discretized in the form of a nonlinear vector equation parametrized by the Reynolds number,

$$\boldsymbol{f}(\boldsymbol{w}, Re) = \boldsymbol{0}; \qquad \boldsymbol{f} : \mathbb{R}^N \times \mathbb{R} \mapsto \mathbb{R}^N \tag{4}$$

where $\mathbb{R}^N$ is the set of real vectors of dimension N. In the implementation reported here, isoparametric quadrilateral elements were used with biquadratic interpolation of the velocity field and discontinuous linear interpolation of the pressure field. The vector $\boldsymbol{w}$ defines the discretized velocity and pressure fields. Solutions to Eq. (4) are found by a Newton iteration.

Provided the finite element mesh is symmetric about $y = 0$, an argument paralleling that provided by Cliffe and Spence,[14,15] shows that the nonlinear system of Eq. (4) is equivariant with respect to an $(n \times n)$ orthogonal matrix S, where $S^2 = I$ and $S \neq I$, i.e.,

$$S\,\boldsymbol{f}(\boldsymbol{w}, Re) = \boldsymbol{f}(S\boldsymbol{w}, Re) \tag{5}$$

The action of the matrix S on the vector $\boldsymbol{w}$ is to replace the streamwise velocity component $u(x, y)$ with $u(x, -y)$, the cross-stream velocity component $v(x, y)$ with $-v(x, -y)$, and the pressure $p(x, y)$ with $p(x, -y)$.

The matrix S induces a unique decomposition of $\mathbb{R}^N$ into symmetric and antisymmetric subspaces, $\mathbb{R}^N = \mathbb{R}^N_s \oplus \mathbb{R}^N_a$, where

$$\mathbb{R}^N_s = \{\boldsymbol{w} \in \mathbb{R}^N : S\boldsymbol{w} = \boldsymbol{w}\}$$

$$\mathbb{R}^N_a = \{\boldsymbol{w} \in \mathbb{R}^N : S\boldsymbol{w} = -\boldsymbol{w}\}$$

A symmetric flow is one for which $\boldsymbol{w} \in \mathbb{R}^N_s$, so at any downstream location x, the streamwise components of velocity at an equal distance from but on opposite sides of the centerline are equal, i.e., $u(x, y) = u(x, -y)$. The cross-stream components of velocity at an equal distance from but on opposite sides of the centerline have opposite sign, i.e., $v(x, y) = -v(x, -y)$, and the pressure components are equal i.e., $p(x, y) = p(x, -y)$. The flow shown in Fig. 2a possesses this symmetry, whereas the flow shown in Fig. 2b does not.

At a regular point $(\boldsymbol{w}_0, Re_0)$ of Eq. (4), $\boldsymbol{f}(\boldsymbol{w}_0, Re_0) = \boldsymbol{0}$ and the Jacobian

$$\left.\frac{\partial \boldsymbol{f}}{\partial \boldsymbol{w}}\right|_{(\boldsymbol{w}_0, Re_0)} = \boldsymbol{f}_{\boldsymbol{w}}(\boldsymbol{w}_0, Re_0) = \boldsymbol{f}^0_{\boldsymbol{w}}$$

is nonsingular. The implicit function theorem guarantees a unique branch of solutions to Eq. (4) passing through $(\boldsymbol{w}_0, Re_0)$ parametrized by the Reynolds number.

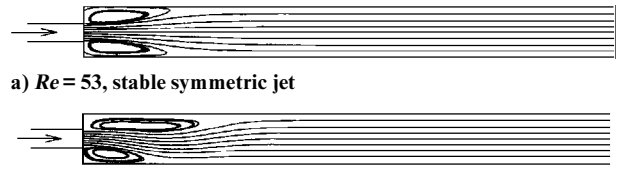

a) $Re = 53$, stable symmetric jet

b) $Re = 67$, stable asymmetric jet

Fig. 2 Streamlines for $D/d = 3$.

At a simple singular point $(\boldsymbol{w}_c, Re_c)$ of Eq. (4), $\boldsymbol{f}(\boldsymbol{w}_c, Re_c) = \boldsymbol{0}$, but the Jacobian matrix $\boldsymbol{f}^c_{\boldsymbol{w}} = \boldsymbol{f}_{\boldsymbol{w}}(\boldsymbol{w}_c, Re_c)$ is singular, and

$$\begin{aligned} \text{Null}(\boldsymbol{f}^c_{\boldsymbol{w}}) &= \text{span}\{\boldsymbol{\phi}_c\}, \qquad \boldsymbol{\phi}_c \in \mathbb{R}^N \\ \text{Range}(\boldsymbol{f}^c_{\boldsymbol{w}}) &= \{\boldsymbol{y} \in \mathbb{R}^N : \langle \boldsymbol{\psi}_c, \boldsymbol{y} \rangle = 0,\ \boldsymbol{\psi}_c \in \mathbb{R}^N\} \end{aligned} \tag{6}$$

where $\langle \cdot, \cdot \rangle$ denotes the inner product. A unique branch of solutions passing through $(\boldsymbol{w}_c, Re_c)$ can no longer be guaranteed. If $\boldsymbol{w}_c \in \mathbb{R}^N_s$ and $\boldsymbol{\phi}_c \in \mathbb{R}^N_a$, a pitchfork bifurcation point occurs at $(\boldsymbol{w}_c, Re_c)$ (e.g., Ref. 16). Pitchfork bifurcation points that occur as a result of symmetry breaking of the type described earlier (Z_2-symmetry breaking) may be computed as regular points (isolated solutions) of the $(2N + 1)$-dimensional extended system proposed by Werner and Spence,[17] which is

$$\boldsymbol{g}(\boldsymbol{z}) = \begin{pmatrix} \boldsymbol{f} \\ \boldsymbol{f}^{\phi}_{\boldsymbol{w}} \\ \langle \boldsymbol{l}, \boldsymbol{\phi} \rangle - 1 \end{pmatrix} = \boldsymbol{0} \tag{7}$$

where

$$\boldsymbol{z} = \begin{pmatrix} \boldsymbol{w} \\ \boldsymbol{\phi} \\ Re \end{pmatrix}, \qquad \boldsymbol{z} \in (\mathbb{R}^N_s \times \mathbb{R}^N_a \times \mathbb{R})$$

$$\boldsymbol{g} : \mathbb{R}^N_s \times \mathbb{R}^N_a \times \mathbb{R} \longrightarrow \mathbb{R}^N_s \times \mathbb{R}^N_a \times \mathbb{R}$$

and $\boldsymbol{l} \in \mathbb{R}^N_a \neq \boldsymbol{0}$.

Solutions to Eq. (7), call them $\boldsymbol{z}^T_c = (\boldsymbol{w}^T_c, \boldsymbol{\phi}^T_c, Re_c)$, clearly satisfy the discretized Navier–Stokes equations [Eq. (4)], i.e., $\boldsymbol{f}(\boldsymbol{w}_c, Re_c) = \boldsymbol{0}$, and $\boldsymbol{w}_c$ is required to be symmetric with respect to S. Simultaneously $(\boldsymbol{w}_c, Re_c)$ is required to be a singular point of Eq. (4), because $\boldsymbol{f}_{\boldsymbol{w}}(\boldsymbol{w}_c, Re_c)$ must possess a nontrivial null eigenvector $\boldsymbol{\phi}_c$ that further is antisymmetric with respect to S. From a solution of Eq. (7), we therefore obtain the critical Reynolds number at the pitchfork bifurcation point, the discretized solution at the bifurcation point, and the discretized null eigenvector. We know from singularity theory that there are nearby solutions of the form $\boldsymbol{w}_c \pm \epsilon \boldsymbol{\phi}_c + \mathcal{O}(\epsilon^2)$ for small enough ϵ. Thus $\boldsymbol{w}_c \pm \epsilon \boldsymbol{\phi}_c$ can be used as initial guesses for a Newton iteration to find solutions on the two asymmetric branches of solutions to Eq. (4), which develop (in this instance supercritically) from the pitchfork bifurcation point. As shown by Cliffe and Spence,[14] it is possible to construct both $\boldsymbol{w} \in \mathbb{R}^N_s$ and $\boldsymbol{\phi} \in \mathbb{R}^N_a$ and compute the necessary integrals to construct Eq. (7) on only half of the domain shown in Fig. 1, representing a considerable savings in computational expense.

The linear stability of the asymmetric flows was determined for a range of Reynolds numbers. The standard linear stability development applied to solutions of the Navier–Stokes equations discretized using a mixed finite element method produces a large sparse nonsymmetric generalized eigenvalue problem. We used the Cayley transform techniques developed by Cliffe et al.[18] coupled with subspace iteration to find the eigenvalue(s) with the smallest real part. All the features described earlier are implemented within the code ENTWIFE.[19]

III. Discussion of Results

The laminar flow in two-dimensional symmetric channels has been observed to change from a stable symmetric jet to a stable asymmetric jet with increasing Reynolds number.[1–6] This change

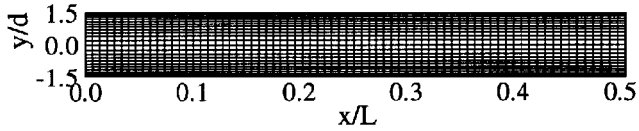

Fig. 3 Rectangular grid of 256 × 111 grid points showing every second node in *x* and fourth node in *y*, where *L* = 50*d*.

occurs at a symmetry-breaking bifurcation point[4] where the solution set changes from a single, stable symmetric flow to two stable asymmetric flows (corresponding to the jet bending towards either wall) and an unstable symmetric flow. The critical Reynolds number is a function of the expansion ratio.

The critical Reynolds number corresponding to the symmetry-breaking bifurcation can not be numerically simulated, however, because simulations close to the bifurcation become computationally very intensive. Instead, symmetric and asymmetric flows on either side of the bifurcation were computed yielding an ever-decreasing range of Reynolds numbers in which the bifurcation must occur. A rectangular grid was used in the numerical simulations with clustering close to the walls (see Fig. 3 for a partial view of the grid). It was determined that simulations computed on a grid of at least 256 × 111 yielded grid-independent results, where overall accuracy was believed to be within 1%. Depending on the length of the channel, a mesh composed of 256 × 111 grid points or 512 × 111 grid points was used. A typical grid aspect ratio $\Delta y/\Delta x$ was on the order of 0.2. The criterion for convergence was that changes in the solution between each real time step be on the order 10^{-10}.

Numerical bifurcation techniques can locate singularities of the discretized steady Navier–Stokes equations. The critical Reynolds number at the symmetry-breaking bifurcation point was computed as part of a regular (isolated) solution to the Werner–Spence extended system [Eq. (7)]. Results were checked for sensitivity with respect to the discretization and domain length. The domain was always long enough to capture all of the significant components of the null eigenvector and to ensure recovery of the Poiseuille parabolic velocity profile at the downstream boundary. The symmetry-breaking bifurcation points reported here were computed on a grid with more than 60,000 degrees of freedom on one-half of the domain shown in Fig. 1. The critical Reynolds numbers are believed to have converged to within 1% in all cases.

Figure 2a is a streamline plot of the stable symmetric solution for $D/d = 3$ and $Re = 53$. As the Reynolds number is increased further, the symmetry-breaking bifurcation occurs. Streamlines of one of the two possible asymmetric flows at $Re = 67$ are shown in Fig. 2b. The full length of the channel has not been shown; however, as can be seen from the horizontal streamlines, the flow is essentially parallel to the channel walls at a distance of 30 inlet heights downstream of the expansion. Furthermore, the values of the streamlines have been chosen so that they are equally spaced for a fully developed parabolic flow.

Numerical simulations using the time-accurate formulation have proven to be an efficient method for locating this symmetry-breaking bifurcation point, even though the resulting numerical solutions are all steady. Bifurcation calculations of the critical Reynolds number at the symmetry-breaking bifurcation were performed for expansion ratios $D/d = 1.5$, 2, 3, 4, 5, and 7. There is clearly an inverse relationship between expansion ratio and critical Reynolds number. A summary of the predictions using bifurcation calculations and the simulations are presented in Table 1. Also cited in the table are data from other published work, where the Reynolds numbers and expansion ratios have been redefined to be consistent with this paper.

The velocity and pressure components of the null eigenvector at the pitchfork bifurcation point computed as part of a regular (isolated) solution of Eq. (7) are shown in Figs. 4a–4c. In these figures the cross-stream direction has been expanded by a factor of 3. The eigenvector is antisymmetric with respect to the matrix S because at any downstream location x the streamwise velocity components at an equal distance from but on opposite sides of the centerline, i.e., at (x, y) and $(x, -y)$, have the same magnitude but opposite sign. The cross-stream velocity components of the eigenvector at (x, y) and $(x, -y)$ are equal both in magnitude and sign, whereas

Table 1 Comparison of simulations, bifurcation calculations, and experimental data

	Re_c		
D/d	Simulations	Bifurcation calculations	Experimental data
1.5	——	297.5	——
2	150–155	143.6	
	83.3[6]	143[5]	100–123[2]
3	57–58	53.8	——
	——	55[5]	44[4]
4	35–40	35.8	——
5	27–30	28.4	30[3]
7	——	10.73	——

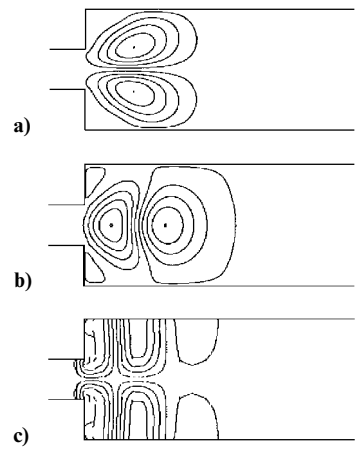

Fig. 4 Null eigenvector components for the a) streamwise velocity, b) cross-stream velocity, and c) pressure.

the pressure components of the eigenvector have equal magnitude but opposite sign. As previously reported by Shapira et al.,[5] a linear stability analysis about the symmetric solutions shows that at the symmetry-breaking bifurcation point a real eigenvalue of the resulting generalized eigenvalue problem crosses into the unstable left half of the complex plane, where the corresponding null eigenvector is as shown in Figs. 4a–4c. Computation of terms involving higher-order derivatives[15] confirmed the supercritical nature of the symmetry-breaking bifurcation for all expansion ratios studied.

It has been widely reported that the asymmetric flows become unsteady at higher Reynolds numbers. Based upon a linear stability analysis about the asymmetric flows, we believe these flows remain stable with respect to two-dimensional disturbances beyond the Reynolds number at which unsteady flows are reported by Fearn et al.[4] The time-dependent motions observed by these authors are therefore presumed to be three dimensional in nature.

The velocity profiles measured by Fearn et al.[4] are compared with our computations for the expansion ratio $D/d = 3$. Figure 5a is a streamline contour plot for $Re = 80$ with the flow attached to the bottom wall. At this Reynolds number, two recirculation regions form downstream of the expansion. Figure 5b is a plot of the streamwise velocity profiles compared at four streamwise locations, which are also indicated for reference in Fig. 5a. Figures 6a and 6b show similar information for $Re = 187$. Figure 6a shows that the flow initially attaches to the lower wall. It can be seen from the streamline contours that at a higher Reynolds number a third recirculation zone has developed downstream. The jet separates from the lower wall, impinges on the upper wall, and then reattaches to the lower wall. Both Figs. 5b and 6b show that farther downstream at streamwise locations $x/d = 20$ and 40, respectively, the flowfield has a symmetric profile indicating the flow has returned to a parabolic distribution. Overall, the simulations and finite element calculations are in good agreement with the experimental data.

The transition from a stable symmetric flow to an asymmetric flow is illustrated by the bifurcation diagram shown in Fig. 7. The cross-stream velocity along the centerline of the channel provides a convenient norm of the solution since it is zero for a symmetric flow and nonzero with opposite signs for the two possible asymmetric

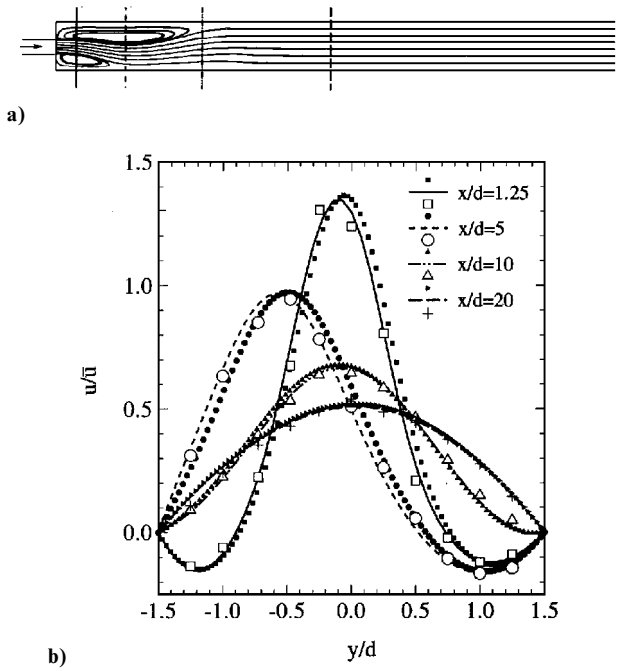

Fig. 5 Asymmetric jet at $Re = 80$ for $D/d = 3$ showing a) streamline contours and b) streamwise velocity profile comparisons of the simulations (solid symbols), bifurcation calculations (lines), and experiments (open symbols).

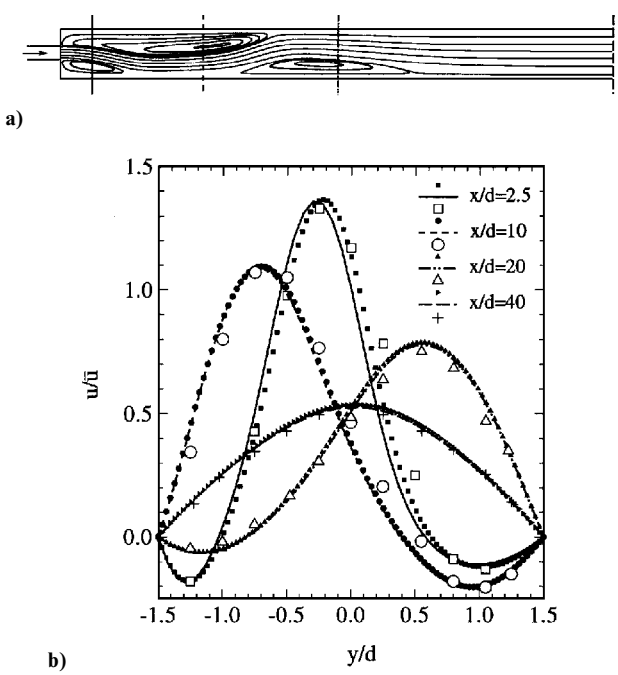

Fig. 6 Asymmetric jet at $Re = 187$ for $D/d = 3$ showing a) streamline contours and b) streamwise velocity profile comparisons of the simulations (solid symbols), bifurcation calculations (lines), and experiments (open symbols).

flows. Because of experimental constraints, Fearn et al.[4] took measurements at 25.5 mm downstream of the expansion along the centerline of the channel and compared their numerical calculations at the same location. The upper branch corresponds to flow attaching to the upper wall and the lower branch corresponds to the flow that is the mirror image about the centerline of the channel. Fearn et al. calculated $Re_c = 54$ for $D/d = 3$, using an earlier version of the present code ENTWIFE.[19]

The cross-stream velocity measurements at 25.5 mm are seen to decrease beyond a Reynolds number of 70 and change sign near $Re = 130$. The maximum value of the cross-stream velocity along

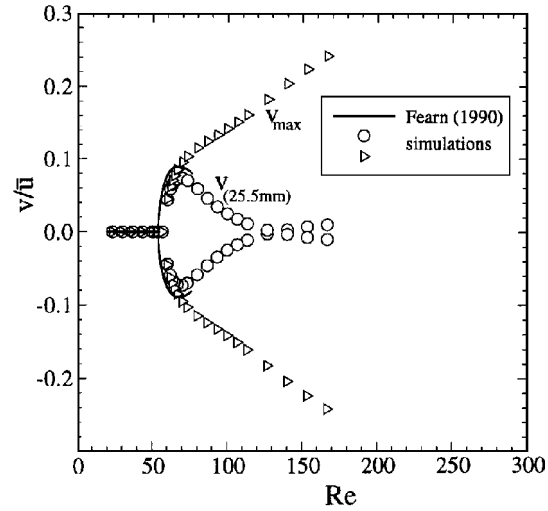

Fig. 7 Comparison of the simulations and bifurcation calculations of Fearn et al.[4]

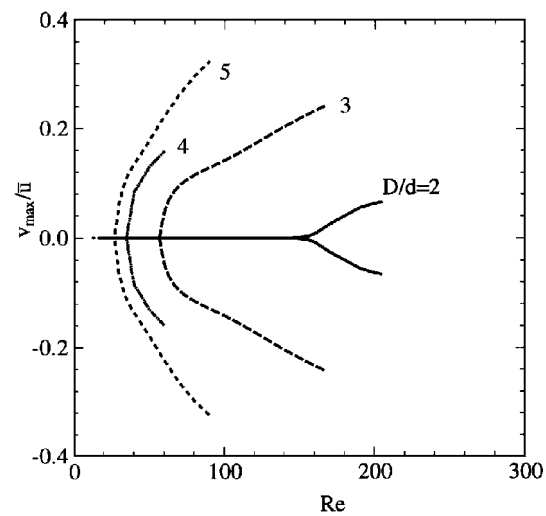

Fig. 8 Numerical simulations of the symmetry-breaking pitchfork bifurcation at expansion ratios $D/d = 2$, 3, 4, and 5.

the centerline provides another norm of the solution and is indicated by triangles in Fig. 7. This norm shows more clearly how the asymmetry increases with Reynolds number. The bifurcation diagrams produced by plotting the maximum value of the cross-stream velocity along the centerline against the Reynolds number are shown in Fig. 8 for a range of expansion ratios.

The presence of perturbations that do not preserve the midplane symmetry, which occur inevitably in any experimental apparatus, disconnect the pitchfork bifurcation as discussed, for example, by Golubitsky and Schaeffer.[16] The disconnectionof pitchfork bifurcation when perfect midplane symmetry is not attained has been recognized by Fearn et al.,[4] who observed that significant asymmetries were present in the experimental flow at $Re = 44$, a value well below the critical Reynolds number in a symmetric two-dimensional domain. They also show that the disconnected branch has a lower limit of stability, presumably at a turning point, which is the codimension-zero singularity in the absence of symmetry. They further showed that a perturbation of only 1% could be responsible for such a large disconnection. We note that the experimental values for a 1:2 channel expansion ratio reported by Cherdron et al.[2] also significantly underestimate the computed stability limit of the symmetric flow in a symmetric domain, and we believe that this arises from the same cause.

For an expansion ratio $D/d = 5$ we compare our results to the experimental work of Ouwa et al.[3] The critical Reynolds number

was experimentally found to be 30. The simulations indicate Re_c just under 30, and bifurcation calculations predicted $Re_c = 28.4$, which compares well with the experiments. Ouwa et al. also investigated whether there were any hysteretic effects associated with the transition. By first starting with a symmetric flow, the Reynolds number was increased above the critical Reynolds number. With an already asymmetric flow, the Reynolds number was decreased below the critical value. They found that the transition occurred near $Re = 30$, regardless of whether the Reynolds number was decreased or increased. While hysteretic phenomena may arise from the two-parameter unfolding of a pitchfork bifurcation point,[16] it was not observed by Fearn et al.[4] and indeed occurs in a small region of the unfolding-parameter space, and its absence is not surprising.

The bifurcation can also be illustrated by considering how the flow reattaches to the channel walls for symmetric and nonsymmetric flows. A schematic of the nozzle is shown in Fig. 9 indicating the primary and secondary attachment positions along the nozzle walls, where x_n are primary attachments and x_0^m are secondary attachments. It was observed that increasing the Reynolds number increased the number of primary attachment points of an asymmetric jet. The primary attachment positions for $D/d = 3$ and 5 are shown in Fig. 10. Initially, at very low Reynolds numbers, the primary attachment positions x_1 and x_2 are equal, indicating symmetric flow. At a critical Reynolds number there is a branching that indicates asymmetric flow for which the nearer attachment position, x_2, remains relatively constant, while the attachment position on the opposite channel wall, x_1, starts to increase monotonically. The recirculation region defined by x_1 continues to grow at the expense of the other recirculation zone x_2. A third recirculation region develops with further increases in Reynolds number, represented by attachment positions x_3 and x_4. This qualitative change in the streamline pattern is not associated with a bifurcation point of the Navier–Stokes equations. Similar behavior has been observed by Chen et al.[20] in the flow past a cylinder and by Goodwin and Schowalter[21] in expanding channel flows with twin inlets.

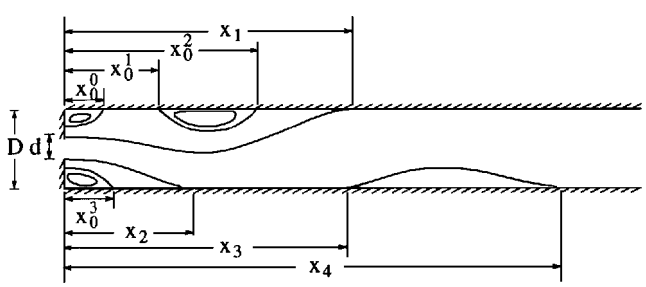

Fig. 9 Schematic of primary and secondary attachment positions assuming jet initially deflects toward lower wall.

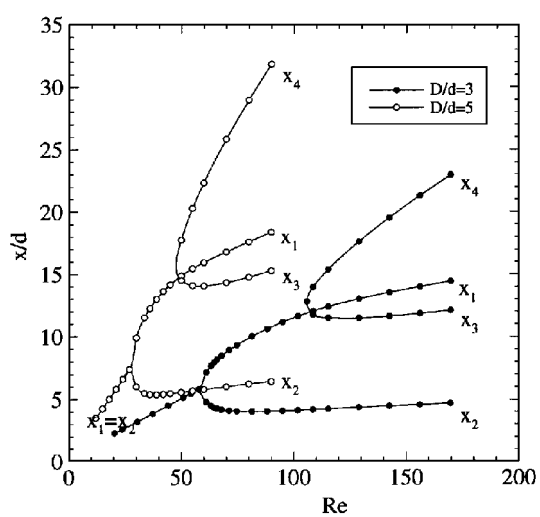

Fig. 10 Primary attachment positions for $D/d = 3$ and 5.

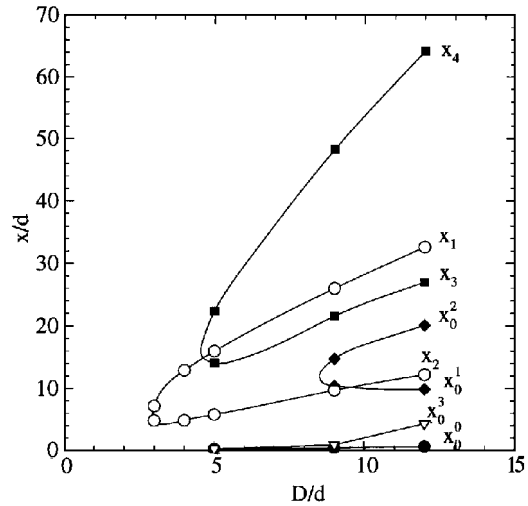

Fig. 11 Primary and secondary attachment positions for $Re = 60$.

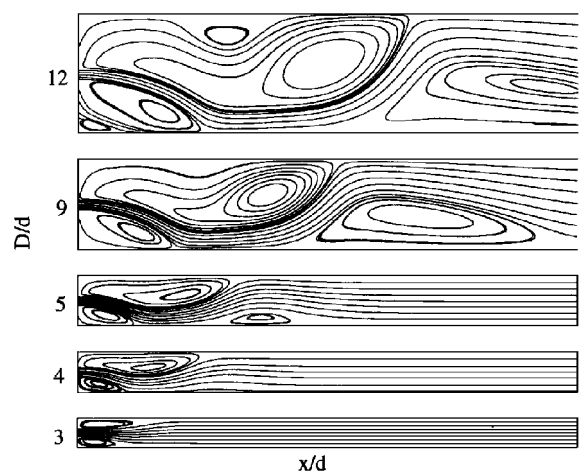

Fig. 12 Streamline contours for expansion ratios $D/d = 3$, 4, 5, 9, and 12 at $Re = 60$ and domain length $x/d = 50$.

The attachment positions can also be examined by varying the expansion ratio at a fixed Reynolds number. Figure 11 is a plot of the attachment positions against the expansion ratio D/d at $Re = 60$ and indicates an approximately linear relationship between the expansion ratio and the primary attachment positions. It can be seen that the distance between lines of x_0^1, x_0^2 and x_3, x_4 represent the lengths of the recirculation zones. As the expansion ratio is increased, smaller recirculation regions are visible in the corners immediately following the expansion, shown as positions x_0^0 and x_0^3. Figure 12 shows the streamlines at $Re = 60$ for the different expansion ratios plotted on a domain of length $x/d = 50$. The growth of the secondary recirculation zones can also be seen for $D/d = 9$ and 12. (Longer domains were used for $D/d = 9$ and 12 than are shown in Fig. 12.)

IV. Conclusions

Numerical simulations and bifurcation calculations were conducted for flow in a two-dimensional channel with a sudden symmetric expansion. A symmetry-breaking bifurcation was found at low Reynolds numbers, representing transition from a symmetric to an asymmetric developing jet. The critical Reynolds number at the bifurcation point was determined for various expansion ratios. Although under ideal conditions of exact midplane symmetry, the transition occurs abruptly at the critical Reynolds number at a symmetry-breaking pitchfork bifurcation point, it is disconnected in the presence of perturbations that do not preserve the midplane symmetry. It was shown that the critical Reynolds number decreased with increasing expansion ratio. The results of numerical simulations and

computations of the bifurcation points were found to be in good agreement with each other and with experimental work.

Our results also show that for a fixed expansion ratio increasing the Reynolds number increases the number of attachment positions for an asymmetric jet. There is also evidence that for a fixed Reynolds number an approximately linear relationship exists between the expansion ratio and the downstream location of the primary reattachment points.

The results of our two-dimensional analysis cannot be applied directly to the analogous three-dimensional flow in a cylindrical pipe that undergoes a sudden symmetric expansion. In the axisymmetric domain, flow at low Reynolds number is described by the symmetry group of a circle, rather than the reflectional symmetry about the midplane of planar channel flow. The possible ways in which these two different symmetries may be broken are qualitatively different. The basic instability mechanism observed in two dimensions could quite conceivably operate to produce steady asymmetric jets in an expanding pipe. However, on the basis of two-dimensional computations and abstract singularity theory alone, we cannot determine whether such an instability occurs. The answer to this question is being sought using both the finite difference and finite element approaches described in this paper.

Acknowledgments

The authors would like to thank the Center for Academic Computing at the Pennsylvania State University for the computing time made available on the IBM RS/6000 SP. We extend our gratitude to Jinzhang Feng for his computer code, which was used for the numerical simulations. In addition, we would like to thank Thomas Mullin of Oxford University for sending us original figures containing the data mentioned in this paper.

References

[1]Durst, F., Melling, A., and Whitelaw, J. H., "Low Reynolds Number Flow over a Plane Symmetric Sudden Expansion," *Journal of Fluid Mechanics*, Vol. 64, Pt. 1, 1974, pp. 111–128.

[2]Cherdron, W., Durst, F., and Whitelaw, J. H., "Asymmetric Flows and Instabilities in Symmetric Ducts with Sudden Expansions," *Journal of Fluid Mechanics*, Vol. 84, Pt. 1, 1978, pp. 13–31.

[3]Ouwa, Y., Watanabe, M., and Asawo, H., "Flow Visualization of a Two-Dimensional Water Jet in a Rectangular Channel," *Japanese Journal of Applied Physics*, Vol. 20, No. 1, 1981, pp. 243–247.

[4]Fearn, R. M., Mullin, T., and Cliffe, K. A., "Nonlinear Flow Phenomena in a Symmetric Sudden Expansion," *Journal of Fluid Mechanics*, Vol. 211, 1990, pp. 595–608.

[5]Shapira, M., Degani, D., and Weihs, D., "Stability and Existence of Multiple Solutions for Viscous Flow in Suddenly Enlarged Channels," *Computers and Fluids*, Vol. 18, No. 3, 1990, pp. 239–258.

[6]Durst, F., Pereira, J. C. F., and Tropea, C., "The Plane Symmetric Sudden-Expansion Flow at Low Reynolds Numbers," *Journal of Fluid Mechanics*, Vol. 248, 1993, pp. 567–581.

[7]Luxton, R. E., and Nathan, G. J., "A Precessing Asymmetric Flow Field in an Abrupt Expanding Axi-Symmetric Duct," *10th Australasian Fluid Mechanics Conference*, Univ. of Melbourne, Australia, 1989, pp. 11.29–11.32.

[8]Nathan, G. J., "The Enhanced Mixing Burner," Ph.D. Thesis, Dept. of Mechanical Engineering, Univ. of Adelaide, Australia, 1988.

[9]Chorin, A., "A Numerical Method for Solving Incompressible Viscous Flow Problems," *Journal of Computational Physics*, Vol. 2, Aug. 1967, pp. 12–26.

[10]Battaglia, F., "Numerical Simulations of Instabilities and Asymmetric Characteristics for Suddenly Expanded Channel Flows," Ph.D. Thesis, Dept. of Mechanical Engineering, Pennsylvania State Univ., University Park, PA, Dec. 1996.

[11]Venkateswaran, S., and Merkle, C. L., "Dual Time Stepping and Preconditioning for Unsteady Computations," AIAA Paper 95-0078, Jan. 1995, pp. 1–14.

[12]Schwer, D. A., Tsuei, H.-H., and Merkle, C. L., "Computation and Validation of Spatially Developing Reacting Mixing Layers," AIAA Paper 95-0261, Jan. 1995.

[13]Gunzburger, M. D., *Finite Element Methods for Viscous Incompressible Flows*, Academic, San Diego, 1989.

[14]Cliffe, K. A., and Spence, A., "The Calculation of High Order Singularities in the Finite Taylor Problem," *Numerical Methods for Bifurcation Problems*, Birkhäuser–Verlag, Heidelberg, Germany, 1984, pp. 129–144.

[15]Cliffe, K. A., and Spence, A., "Numerical Calculations of Bifurcations in the Finite Taylor Problem," *Numerical Methods for Fluid Dynamics II*, Clarendon, Oxford, England, UK, 1986, pp. 177–197.

[16]Golubitsky, M., and Schaeffer, D. G., *Singularities and Groups in Bifurcation Theory*, Vol. 1, Applied Mathematical Sciences, Springer–Verlag, New York, 1985.

[17]Werner, B., and Spence, A., "The Computation of Symmetry-Breaking Bifurcation Points," *SIAM Journal on Numerical Analysis*, Vol. 21, No. 2, 1984, pp. 388–399.

[18]Cliffe, K. A., Garratt, T. J., and Spence, A., "Eigenvalues of the Discretized Navier-Stokes Equation with Application to the Detection of Hopf Bifurcations," *Advances in Compututional Mathematics*, Vol. 1, No. 1, 1993, pp. 337–356.

[19]Winters, K. H., "ENTWIFE User Manual (Release 1)," Theoretical Physics Div., Harwell Lab., Harwell Rept. AERE-R 11577, Oxford, England, UK, May 1985.

[20]Chen, J.-H., Pritchard, W. G., and Tavener, S. J., "Bifurcation for Flow Past a Cylinder Between Parallel Plates," *Journal of Fluid Mechanics*, Vol. 284, 1995, pp. 23–41.

[21]Goodwin, R. T., and Schowalter, W. R., "Arbitrarily Oriented Capillary-Viscous Planar Jets in the Presence of Gravity," *Physics of Fluids*, Vol. 7, No. 5, 1995, p. 954.